TWO-DIMENSIONAL MODELS FOR STEP DYNAMICS

John D. Weeks, Da-Jiang Liu, Hyeong-Chai Jeong
Institute for Physical Science and Technology
University of Maryland, College Park, Maryland 20742
(From *Dynamics of Crystal Surfaces and Interfaces*, eds. P.M. Duxbury and T. Pence, Plenum Press, New York, 1997)

1 INTRODUCTION

In this paper we review some of our recent work on the dynamics of step bunching and faceting on vicinal surfaces below the roughening temperature, concentrating on several cases where interesting two dimensional (2D) step patterns form as a result of kinetic processes. We show that they can be understood from a unified point of view, based on an approximate but physically motivated extension to 2D of the kind of 1D step models studied by a number of workers. For some early examples, see refs. [1-5]. We have tried to make the conceptual and physical foundations of our own approach clear, but have made no attempt to provide a comprehensive review of work in this active area. More general discussions from a similar perspective and a guide to the literature can be found in recent reviews by Williams[6] and Williams and Bartelt[7].

We consider conditions where there is no significant island or void nucleation on the terraces, and surface mass transport is associated with the addition and removal of material from the preexisting surface steps. This provides an important simplification since the number of steps is now a conserved quantity and we do not have to deal with problems arising from the annihilation of steps of different sign.

We operate on a *mesoscopic* scale, intermediate between the atomic scale and continuum theory, taking individual surface steps as the fundamental objects of interest. One way to achieve this is to imagine an anisotropic coarse-graining of the surface much like that produced in REM experiments[8]. We average along the nominal step direction (the y-direction) to a scale large compared to the atomic scale but small compared to the step patterns of interest, while maintaining an atomic scale resolution normal to the steps (the steps ascend in the x-direction) and in the z-direction. When viewed from above, smooth long wavelength configurations of steps and terraces can be resolved but not microscopic objects like adatoms and kinks.

This scale is directly relevant to STM and REM experiments, and we believe it offers significant theoretical advantages over approaches that consider a more general coarse-graining using the step density as a variable. We can provide a more intuitive and physically motivated description of changes in the surface morphology using the basic entity involved, the step. Moreover, we can examine the properties of individual steps as they move and bunch together and the step patterns that form.

To proceed, we must describe the effective driving force and the effective interactions between steps on this mesoscopic scale. We focus here on two cases of recent experimental and theoretical interest: current-induced step bunching on Si(111) surfaces[8–10] and reconstruction-induced faceting as seen a number of systems including the O/Ag(110) and Si(111) surfaces[11,12]. In both cases interesting 2D step patterns can arise from the competition between a driving force that promotes step bunching, and the effects of step repulsions, which tend to keep steps uniformly spaced.

2 TREATMENT OF STEP REPULSIONS AND FLUCTUATIONS

2.1 Physical origin

We first discuss the simpler situation that arises in the *absence* of the driving force, where the physics is dominated by the effects of step repulsions. The resulting equations can describe, e.g., the relaxation of initially nonuniform step configurations towards the equilibrium state[13,14]. The origin of the repulsive step interactions can be understood from the following. Although steps of the same sign can in principle bunch together, possibly even producing multiple-height steps, transverse fluctuations of a step in such a bunch are suppressed because of the prohibitively high energy cost associated with step crossings or overhangs. On averaging or coarse-graining, these constrained arrangements have a lower entropy (higher free energy) than that found when steps are further apart. This produces an (entropically-driven) effective *repulsion* between steps in the coarse-grained model, which favors uniform step spacing at equilibrium[6].

Fluctuations of an isolated step are also suppressed by the microscopic energy cost to form kinks. On coarse-graining, this translates into an effective *stiffness* or *line tension* that tends to keep the step straight. Standard microscopic 2D models of step arrays incorporating both of these physical effects include the free-fermion model and the Terrace-Step-Kink (TSK) model[5,15]. Both models have proved very useful, though their microscopic nature makes detailed calculations difficult.

Perhaps the most important conclusion arising from

a study of such models is that the projected free energy density[1] of a *uniform* vicinal surface with slope s is given by the familiar Gruber-Mullins[16] expression:

$$f(s) = f^0 + \frac{\beta}{h}s + gs^3 . \qquad (1)$$

Here f^0 is the free energy density of the flat surface, β the creation energy per unit length of an isolated step of height h (taken as the unit of length hereafter) and g the step interaction parameter, whose magnitude in general takes account of both entropic and possible direct elastic interactions. Eq. (1) can equally well be thought of as describing the free energy in a 1D model of straight uniformly spaced steps with effective repulsive interactions, or as the free energy in a 2D model where all steps are in their straight average (equilibrium) positions.

2.2 Step Hamiltonian for repulsive interactions

Our goal here is to provide a simpler 2D description of the mesoscopic scale physics, consistent with Eq. (1), in a form useful for practical calculations. To that end, in analogy with density functional methods for inhomogeneous fluids[17], we introduce an *intrinsic* (or configurational) *free energy functional* for the stepped surface. This gives the free energy of a macroscopic surface with N_s steps as a functional of the positions $\{x_n(y)\}$ of all the steps.

To obtain a physical picture, imagine first producing a nonuniform step configuration with the aid of an external field. Then the field is turned off. The intrinsic free energy can be crudely thought of as the free energy of such a perturbed system before it relaxes back to the uniform state. Although we will not use it here, the density functional formalism allows for a precise and formally exact treatment of this idea. Arbitrary equilibrium step configurations $\{x_n(y)\}$ can be produced formally by applying an appropriately chosen conjugate external field $\{\phi(x,y)\}$ that couples linearly to the step positions; in the uniform system with straight steps described by Eq. (1), ϕ is zero everywhere. The intrinsic free energy results when the linear contribution to the free energy that depends *explicitly* on the external field is subtracted from the (Helmholtz) free energy of the nonuniform system in the field. Technically, this generates a Legendre transform giving the free energy as a functional of the configurations $\{x_n(y)\}$ rather than the field $\{\phi(x,y)\}$.

In this paper we will not pursue such formal developments any further, and instead use mean field ideas and heuristic arguments to motivate the choice of the appropriate free energy functional. We represent the intrinsic free energy functional in the form of an *effective 2D step Hamiltonian* H and imagine on physical grounds that it has the following form:

$$H(\{x_n\}) = \int dy \sum_n^{N_s} \left[\frac{\tilde{\beta}}{2} \left(\frac{\partial x_n(y)}{\partial y} \right)^2 + V(w_n(y)) \right]. \qquad (2)$$

The summation is over all N_s steps and the integration is over the coarse-grained y-direction. Thus the magnitude of H depends on the particular values of step positions $x_n(y)$ for all N_s steps and for all y positions. The first term on the r.h.s. describes the energetics of distorting an individual step, controlled by a line tension $\tilde{\beta}$. Everything else is incorporated into an *effective step interaction* V, taken here to be a function only of the *local* nearest neighbor terrace widths $w_n(y) \equiv x_{n+1}(y) - x_n(y)$. This seemingly natural approximation can introduce some notable errors in some cases[2] and more general expressions for the interaction can (and often should!) be used. However, this simple form will prove adequate for our purposes here.

We can determine the interaction term V in Eq. (2) through the requirement that H reproduce the macroscopic free energy in Eq. (1) in the limit of straight steps with uniform spacing w. Thus if L_y is the length of the system in the y-direction we require

$$L_y N_s V(w) = L_y N_s w f(1/w). \qquad (3)$$

The l.h.s. simply evaluates H in this limit and the r.h.s. is the surface area $L_y N_s w$ of the flat reference plane times the projected free energy density $f(s)$ for a uniform system with slope $s = 1/w$. Thus we find

$$V(w) = w f(1/w). \qquad (4)$$

We use this simple expression for V in the rest of this paper.

There are several points worth emphasizing. By using Eq. (4) in Eq. (2), we have made a *local* free energy approximation, relating the free energy of each terrace to that of a uniform system, even when neighboring terrace widths can vary. We have also implicitly assumed that the coarse-graining scale in the y-direction is large

[1] This is defined as the surface free energy per unit area projected onto the low index facet plane. The use of the projected free energy allows a direct analogy with the thermodynamics of a liquid-vapor system. See, e.g., Williams et al.[6] for a clear discussion.

[2] In particular, the energetics of the last step in a bunch next to a reconstructed terrace are incorrectly described. For a 2D model with more general step interaction terms that treats these "corner energy" corrections more accurately see Liu and Weeks[18].

enough or that the distortions away from straight steps are small enough that we can use the same functional form to describe repulsive interactions in V in our 2D model as in the 1D model described by Eq. (1). Moreover, we have evaluated this interaction at the same-y position and have used a quadratic approximation for the line tension term. When the steps are relatively straight, these should be reasonable approximations, but we will use them even in more general cases as a physically motivated model.

2.3 Step chemical potential

Near equilibrium, we expect that the dynamics will be controlled by the energetics of small variations of the step positions in Eq. (2). By definition, the change in H to linear order induced by a small variation $\Delta x_n(y)$ in the position of the nth step is

$$\Delta H = \int \left[\frac{\delta H}{\delta x_n(y)}\right] \Delta x_n(y) dy, \tag{5}$$

where $\delta H/\delta x_n(y)$ is the *functional derivative* of H. Although adatoms are not considered explicitly in our coarse-grained model, we physically relate the area change $\Delta x_n(y)dy$ in Eq. (5) generated by the step displacement to the adsorption and emission of atoms at the step edge. Thus if Ω is the area occupied by an atom near the step edge, we define the *step edge chemical potential* $\mu_n(y)$ — the change in free energy per atom for adding atoms to the step at coarse grained position y — as:

$$\begin{aligned}\mu_n(y) &\equiv -\Omega \frac{\delta H}{\delta x_n(y)} \\ &= \Omega[V'(w_n) - V'(w_{n-1}) + \tilde{\beta}\partial^2 x_n/\partial y^2],\end{aligned} \tag{6}$$

where $V'(w)$ is the derivative of $V(w)$ with respect to w. The last line in (6) arises from functionally differentiating Eq. (2), integrating the variation of the $[\partial x_n(y)/\partial y]^2$ term by parts to arrive at the standard form in (6). The term $V'(w_n)$ has dimensions of force per unit length and can be interpreted as an effective *pressure* on the step associated with terrace n. Thus $\mu_n(y)$ depends on the local (linearized) curvature $\partial^2 x_n/\partial y^2$ of the step and on the difference in pressure from terraces behind and in front of the step. Note that constant terms in V and in the pressure V' do not contribute to $\mu_n(y)$.

2.4 Dynamics from step repulsions

We now study the dynamics arising from the step repulsions. While the classic treatment of BCF[19] assumed local equilibrium at step edges, with steps acting as perfect sinks for adatoms, in many cases a different *attachment/detachment rate limited regime* seems more appropriate. Here we assume that the diffusion rate for adatoms on terraces is much larger than the effective adatom exchange rate between step edges and terraces. To model the step motion, we now make a linear kinetics approximation, assuming that the velocity of a step is proportional to the change in free energy[3] produced by its motion. There are then two limiting cases, depending on how the associated mass flow can take place.

2.4.1 Non-local mass exchange The effective mass flow is *non-local* (Case A) when atoms at a step edge can directly exchange with a vapor reservoir (through evaporation-condensation) or with an overall terrace reservoir that forms by fast direct adatom hops between different terraces. In such cases, we assume that step velocity is proportional to the chemical potential difference between the step and the reservoir:

$$\frac{\partial x_n(y)}{\partial t} = \frac{\Gamma_A}{\Omega k_B T}[\mu_n(y) - \mu_{res}], \tag{7}$$

where the proportionality constant is written in terms of Γ_A, the mobility of the step edge, as defined by Bartelt, et al.[20,21]. The chemical potential μ_{res} of the reservoir is set to be zero when there is no net motion of steps. Since atoms from a given step can go to distant regions through the reservoir, we expect that this mass flow will induce no direct correlation between the motion of neighboring steps.

2.4.2 Local mass exchange A second limit arises when the mass movement occurs *locally* through surface diffusion without direct adatom hops between different terraces. Here the effective adatom exchange is between neighboring step positions only. In the limiting case of *local mass exchange* (Case B), the current between step n and step $n+1$ is assumed to be proportional to the difference in step edge chemical potentials $(\mu_n - \mu_{n+1})$; the net velocity of step n is then given by

$$\frac{\partial x_n(y)}{\partial t} = \frac{\Gamma_B}{\Omega k_B T}[\{\mu_n(y) - \mu_{n+1}(y)\} + \{\mu_n(y) - \mu_{n-1}(y)\}], \tag{8}$$

[3]Thermal fluctuations could also be taken into account through the addition of noise, leading to Langevin-type equations like those studied by Bartelt, et al.[20], but in the applications we consider here, the systems are far from equilibrium, either from initial conditions or because of an explicit driving force, so the simpler deterministic equations will prove adequate.

where Γ_B is the step mobility in this conserved model[4]. This causes a *coupling* of the motion of neighboring steps and, as we will see, can produce interesting step patterns in certain cases.

3 RECONSTRUCTION INDUCED FACETING

In the 1D limit, Eqs. (7) and (8) and related equations have been used to analyze the relaxation of non-equilibrium step profiles[13,14] and in a variety of other applications[3,4]. We will not review this work here, but instead turn directly to two cases where characteristic 2D step patterns and step bunching are found as a result of the competition between the step repulsions and a driving force favoring step bunching. Perhaps the simplest application arises as a result of surface reconstruction.

Surface reconstruction or adsorption can often cause a vicinal surface with a single macroscopic orientation to facet into surfaces with different orientations[6]. Generally the reconstruction occurs on a particular low-index "flat" face, and lowers its free energy relative to that of an unreconstructed surface with the same orientation. However the same reconstruction that produces the lower free energy for the flat face generally *increases* the energy of surface distortions such as steps that disturb the reconstruction. Thus reconstruction is often observed only on terraces wider than some *critical terrace width* w_c. When steps are uniformly distributed initially and if w_c is much greater than the average terrace spacing w_a, step fluctuations leading to the formation of a sufficiently wide terrace — a "critical nucleus" — are required for the reconstruction to begin. Continued growth of the reconstructed region can make the vicinal surface facet into a "flat" reconstructed surface and a much more sharply inclined unreconstructed surface with closely bunched steps.

Experimental examples include faceting associated with the 7×7 reconstruction on Si(111) surfaces[11] and with the formation of $(n \times 1)$ oxygen chains on O/Ag(110) surfaces[12]. In both cases, reconstruction has been observed only on large ($w > w_c$) terraces, where the critical width w_c depends on temperature, pressure and some other parameters. However, experiments on these and some other systems such as Pt(111) and Au(111), show a noticeable regularity in the size and spacing of the flat facets[11,22,23], though the extent of the ordering varies from system to system. In any case, it seems hard to reconcile these regularities with a picture of random nucleation of the reconstructed regions.

3.1 Two state critical width model

To begin a theoretical discussion, it is clear that the existence of a sufficiently large reconstructed region can provide a driving force favoring step bunching in unreconstructed regions. The situation is still relatively simple since we can think of the vicinal surface as moving towards a new equilibrium state in the presence of reconstruction. Moreover, we expect that the *fully* reconstructed surface can be described by the same basic formalism involving step repulsions discussed earlier in Sec. 2.4.

The dynamics of the step motion leading to faceting would be very complicated if it were strongly coupled to the dynamics of reconstruction. Fortunately, in most cases the growth of a reconstructed region occurs much more rapidly than the characteristic time for step motion[24]. Thus we will not consider the dynamics of reconstruction explicitly here, and instead use a simple *two state model*[14,25,26] where each terrace is either reconstructed or unreconstructed, depending only on its *local width*. We first examine the consequences of the two state model when steps are straight, and then incorporate it into the 2D step models.

3.2 Free energies incorporating reconstruction

The reconstruction on the only large terraces, observed in experiments, can be understood by assuming that the free energy of the fully reconstructed flat surface has a lower value, ($-\epsilon_r$ per unit area) than the unreconstructed one but effectively a higher energy cost, (ϵ_s per unit length) for forming an isolated step[6,27]. Thus letting the previous free energy expression, Eq. (1), represent the unreconstructed surface (denoted by the subscript u) we assume the fully reconstructed surface is described by

$$f_r(s) = (f_u^0 - \epsilon_r) + (\beta_u + \epsilon_s)s + gs^3 \,. \tag{9}$$

(In principle the g term would also change but this will have little effect on what follows.) The free energy of the fully reconstructed surface, $f_r(s)$, is lower than that of the unreconstructed surface, $f_u(s)$, when the slope s is less than $s_c \equiv \epsilon_r/\epsilon_s$. The thick curve in Fig 1(a), given by

$$\begin{aligned} f(s) &= f_u(s)\,\Theta(s - s_c) + f_r(s)\Theta(s_c - s) \\ &= f_u(s) - \,(1 - s/s_c)\,\epsilon_r\,\Theta(s_c - s), \end{aligned} \tag{10}$$

[4]We follow Nozieres[2], assuming Γ_B is independent of the terrace width, and neglecting possible "Schwoebel" asymmetries in our description of step repulsions. Other choices could be made[3], but few qualitative changes are seen. For our purposes here the main point is to describe step repulsions at short distances in a reasonable way so that step crossing is prevented.

with Θ the unit step function, represents the free energy of a hypothetical macroscopic system in which *all* terraces are reconstructed (unreconstructed) when the *average* slope s is less than (greater than) s_c.

However, the situation of interest involves the presence of both reconstructed and unreconstructed regions. In fact, because of thermal fluctuations in a real system, for given average slope s, there exists a *distribution* of terrace widths around the average terrace width $w = 1/s$. Therefore, even in a surface with average slope larger than s_c, we expect to find some terraces with widths larger than $w_c \equiv 1/s_c$ in a large system. These represent regions where reconstruction would nucleate according to our two state model. If the average terrace width w_a is much smaller than w_c, we may have to wait a long time before fluctuations produce a sufficiently wide terrace. However, after such an event, the "critical nucleus" will continue to grow since the reconstructed surface has the lower free energy. Continued growth of the reconstructed terrace can cause neighboring unreconstructed terraces to become narrower and to form step bunches. At sufficiently long times, the surface will in principle facet into a flat reconstructed surface and a high slope (step-bunched) region as predicted by the thermodynamic tie bar construction (dashed line) shown in Fig. 1.

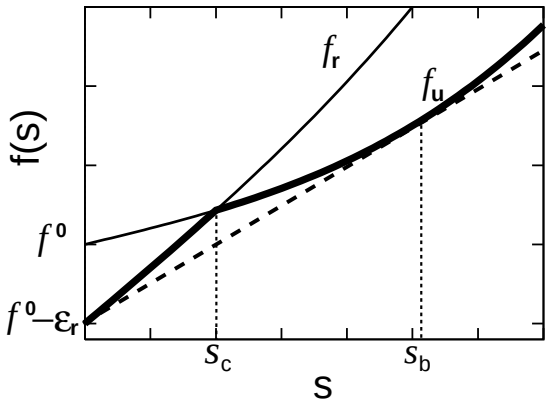

FIG. 1. Free energies for unreconstructed surface f_u and reconstructed surface f_r vs slope s. The critical slope, s_c, and the slope of the surface at step bunches, s_b, are given by $s_c = \epsilon_r/\epsilon_s$ and $s_b = (\epsilon_r/2g)^{1/3}$. The thick curve in (a) represents the free energy of a hypothetical system in which all terraces are reconstructed (unreconstructed) when the average slope, s, is less than (greater than) s_c.

3.3 2D dynamical equations incorporating reconstruction

We now modify the 2D continuum equations of step motion, Eqs. (7) and (8), in order to study some aspects of the dynamics of faceting. We assume the system is in the nucleation regime where the critical width w_c is much larger than the average step spacing w_a. In the simplest approximation discussed here, we incorporate the physics of the two state critical width model into the definition of the effective interaction term $V(w)$ in Eq. (2), which in turn modifies the step chemical potential terms in Eqs. (7) and (8). Again we set $V(w) = wf(1/w)$ as in Eq. (4) but now we use the f from Eq. (10) that takes account of reconstruction if a terrace is sufficiently wide. Note that this use of the two state model to describe an individual terrace with width w is more accurate than is the use of Eq. (10) to describe the properties of a macroscopic surface with average slope $s = 1/w$.

In this model, reconstruction modifies the effective step interactions and thus the dynamics. Both the presence of a reconstructed terrace behind a given step and repulsive entropic or elastic interactions from the step behind make positive contributions to the "pressure" moving the given step forward.

We use this simple model with a fixed w_c only to describe the subsequent growth of an initial reconstructed region created by hand[5]. Starting from the same initial roughly circular nucleus, we numerically integrated the equations of step motion, Eq. (7) and Eq. (8). Thus we can study the continued evolution of the step configurations under the different modes of mass transport. In both cases after a nucleus is created, it grows much faster in the step edge (y) direction (where step repulsions are relatively small) than it does in the normal (x) direction to the steps. Thus the nucleus quickly forms an elongated cigar-like shape. However, the subsequent temporal and spatial behavior of the faceting process is very different depending on the mechanism of mass transport on the surface.

[5]Thermal nucleation cannot be treated properly by the deterministic equations considered here. Even if noise were added, our description of reconstruction using the two state critical width model with fixed w_c is too crude to describe the initial formation of the critical nucleus. However, it does seem adequate to describe the further evolution of the surface once an elongated nucleus has formed. In this context, w_c is the "critical width for continued lateral growth" in y-direction. See Jeong and Weeks[28] for a more satisfactory and general continuum treatment of reconstruction coupled to step motion.

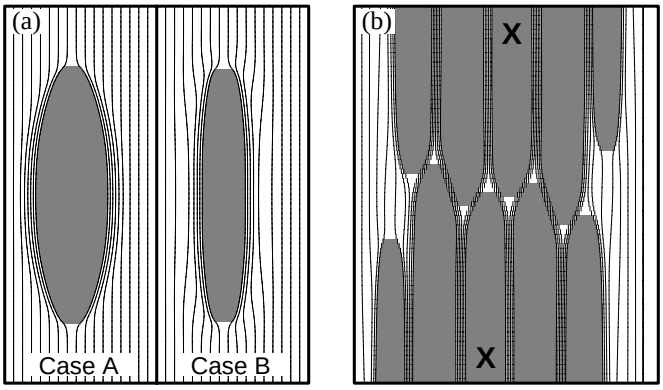

FIG. 2. Top view of step configurations near growing nucleus in the early stage (a) and late stage (b). In (a), initial configurations for both non-local mass exchange of Case A and local mass exchange of Case B are shown. In (b), a regular pattern in Case B arising from interaction between two nuclei through an induced nucleation mechanism is shown. The initial positions of the nuclei (created by hand) are on the terraces marked by X but outside the figure.

Fig. 2 (a) shows typical step configurations from both equations in the early stage of the faceting. In Case A, with non-local mass transport, as the reconstructed facet grows it forces neighboring terraces to become *smaller*. There is a smooth relaxation to the average width far from the facet. Step spacings in case B, with local mass transport, show more interesting behavior because of the correlated step motion. While a region of step bunching is again observed close to the facet, on the other side of the bunch there are also some terraces that are *wider* than average. As the facet continues to grow, the number of steps in the bunched region increases but the widths of the wider terraces in front of the step bunch also increase. One of these may become sufficiently wide to serve as new nucleus for reconstruction. This *induced* nucleation process[25] can repeat itself many times, producing a rather regular pattern of faceted and bunched regions that may be relevant for experiment[29,30]. We will discuss this mechanism in more detail later.

3.4 Isolated facet growth

Before doing this, let us first consider the growth rate of an *isolated* facet. We artificially prevent the formation of other (induced) nuclei on all other terraces by using the free energy curve for the unreconstructed surface regardless of the local terrace width. We then measure the time dependence of the facet length and width during growth. Here, we present only the qualitative results of the study. Quantitative results and the comparison with experiments will be presented elsewhere[26,28].

In both Case A and B, the reconstructed region propagates in y-direction with a constant velocity (after an initial transient where it forms the elongated shape). Thus the lateral size of the facet grows *linearly* with time. Linear growth along the step direction has been seen in experiment already[11] and there are rather general theoretical arguments[26] why it is to be expected.

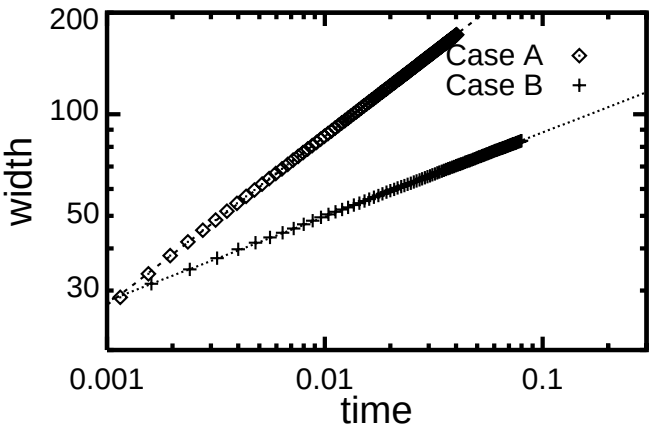

FIG. 3. Measured time dependences of the facet widths for Cases A and B are shown in a log-log plot. All data in each case fall into a line indicating that the reconstructed terrace width increases as $w \sim at^{\alpha}$. The α values of the fitting lines are 1/2 for Case A and 1/4 for Cases B. Time and widths are in arbitrary units.

On the other hand, the growth rate of the *normal* width is different in the two cases. Fig. 3 shows the growth of the facet width versus time in a log-log plot. All data in each case fall into a straight line, indicating that the reconstructed terrace width increases as $w \sim at^{\alpha}$. For case A, the facet grows as $t^{1/2}$, while it grows as $t^{1/4}$ for case B. These results are in complete agreement with the predictions of the classic one-dimensional continuum model of Mullins[31].

3.5 Induced nucleation

Let us now relax the constraint forbidding other nuclei from forming. Even if thermal fluctuations were included, this should produce essentially no change in Case A. Since all terraces near the original facet become smaller on average, other thermally nucleated facets are *less* likely to occur nearby. The story is quite different in Case B with local mass transport, where *induced* nuclei can form and inhibit the further growth of the original facet. In Case B, the motion of a step is directly coupled to the motion of neighboring steps. Initially, as the step bounding the reconstructed terrace moves forward to increase the reconstructed terrace's width, the neighboring step must move backward to conserve adatoms locally. Thus both the original reconstructed terrace and

the terrace in front of the step that moves backward get wider. When the two steps that move in opposite directions come sufficiently close to each other for step repulsions to become important (with spacing approaching that of the equilibrium step bunch), they "collide" and both begin to move forward together as a bunch because of the driving force from the reconstructed terrace behind. Then the local conservation process repeats itself, causing new steps in front of the advancing step bunch to move backward and making the terraces in front of those steps wider. As the original facet grows, the number of steps in the bunch increases and the widths of the widest terraces in front of the step bunch also increase. Such a sufficiently wide terrace can be a nucleus for the reconstruction of another facet.

A quantitative treatment of this induced nucleation mechanism using a 1D model [the $\tilde{\beta} \to \infty$ limit of Eq. (8)] was carried out by Jeong and Weeks[25]. When the typical distance between steps in a step bunch, $w_b \sim (2g/\epsilon_r)^{1/3}$ is much smaller than the average terrace width w_a, it was shown that only one other terrace, aside from the original facet, is larger than w_a at any given time. In the limit that w_b/w_a goes to zero, the maximum width of the induced wide terrace increases *linearly* with the number of steps, n_b, in the bunch separating it from the original facet. Moreover it remains as the widest terrace for an increasing long time interval, $\Delta t \sim n_b^3$. Once it gets larger than w_c, reconstruction will occur. Further growth of the original facet essentially stops, but the new facet can induce another nucleus on the other side as it continues to grow. Then this new nucleus can induce another one and so on. The velocity of the nucleation front is *linear* in time because it always takes the same amount of time to induce a nucleus. Hence the faceted surfaces arising from this idealized process have a periodic distribution of reconstructed terraces separated by step bunches.

3.6 2D patterns from induced nucleation

An interesting 2D pattern arises from induced nucleation using Eq. (8) when two (thermal) nuclei form that are close in the x-direction but separated by a large distance in the y-direction. Fig. 2 (b) shows a step configuration in Case B arising from two such nuclei (created by hand). As time goes, each nucleus grows as $t^{1/4}$ in the normal direction until it produces its own induced nucleus. In the lateral direction, nuclei grow essentially linearly in t until they "collide" with each other and form a bunch of *crossing steps* between them. After such an encounter, the nuclei stop growing in the y-direction. The number of step in a crossing bunch is determined by how many steps initially separated the two nuclei when they formed. Once this configuration forms, other nuclei induced by the two original facets will produce new crossing steps at essentially the same y-position as the original crossing steps. Hence, an *alignment* of crossing step bunches is formed as shown in Fig. 2 (b). The number of steps in the induced crossing bunches are expected to be the same as that in the original crossing step bunch when the idealized induced nucleation mechanism of the 1D model is accurate. A strong tendency for alignment of crossing steps has been found in some step bunching experiments[32] on vicinal GaAs(001) but we do not know whether this is an equilibrium or purely kinetic phenomena as our model would suggest.

If thermal fluctuations were taken into account, the regular patterns selected by this kinetic mechanism would be expected to be less sharp. In particular, when w_b/w_a is not so small, the effects of mass conservation are spread out over many terraces and several terraces in front of the step bunch become larger than w_a. These would be particularly advantageous sites where thermal nucleation could occur, even before the induced width of the terrace as predicted by the deterministic models would exceed w_c. Thus nucleation sites and times are less precisely determined in this case, and we expect the number of steps in a bunch, n_b, to be smaller than the value predicted by the 1D model or the deterministic 2D model. Nevertheless, as calculations with more realistic models show[28], the qualitative feature of the induced nucleation mechanism as discussed here remain valid. While there are a number of different factors (including in particular elastic interactions[22,23]) that can contribute to the facet spacing in particular systems, induced nucleation represents a very general *kinetic* mechanism that should be considered in analyzing experimental data.

4 CURRENT-INDUCED STEP BUNCHING

We now turn to the second main application. Very interesting step bunching instabilities have been seen on vicinal Si(111) surfaces during evaporation by heating with a direct electric current. The direct current heating acts as a driving force producing a net motion of steps as the surface evaporates. Several experimental groups[8–10,33] have shown that the motion of the steps depends crucially on the direction of the current relative to the step orientation. Current in one direction results in stable step flow with uniform step velocities and spacings, while current in the opposite direction causes the steps to bunch together and form complex two dimensional patterns. An electromigration model, involving the diffusion of adatoms (and possibly advacancies[34]) with an effective charge, has been suggested microscopic model. The microscopic physics responsible for the magnitude and sign of the effective charge must be very com-

plicated: there are three temperature regimes where the stable and unstable current directions change roles[38].

Fortunately, many features of the mesoscopic scale physics and the resulting step patterns do not depend on the details of this microscopic physics. Kandel and Weeks[39] (KW) introduced a very successful mesoscopic model describing the step patterns arising from the consequences of a general driving force leading to step bunching and the effects of step repulsions. However, their treatment of the repulsions was rather crude (they imposed a minimal distance requirement by hand) and they made specific physical assumptions (assuming multistep jumps of adatoms over step bunches) whose general applicability could be questioned. Here we show that results essentially identical to those of KW arise very naturally by adding the appropriate driving force terms to the basic equations (7) and (8) describing the effects of repulsive interactions[6]. The situation is both simpler and more complicated than that discussed in Sec. 3, since we do not have the complications of surface reconstruction to contend with, but now the system of interest is continually driven far from equilibrium by the field. As we will see, this reduces the differences between models that assume local and non local mass flow in the treatment of the repulsive interactions.

We adopt the following simple picture. Initially, we assume that steps are far enough apart that the effects of step repulsions can be ignored. The relevant physics for evaporation involves the detachment of adatoms from step edges, their surface diffusion on the adjacent terraces, and their eventual evaporation. This is quite well described by a generalization of the classical BCF model[19], which considers solutions to the adatom diffusion equation with boundary conditions at the step edges.

4.1 Asymmetric velocity function model

The experiments strongly suggest that there is an *asymmetry* in the step-up and step down directions associated with the direction of the electric field. Such an asymmetry can arise both from biased diffusion of adatoms with an effective charge, and by the use of asymmetric kinetic coefficients in the step edge boundary conditions. In a 1D model with straight steps, the result of the generalized BCF model can be expressed quite generally in terms of a set of effective equations of motion for the steps, similar to Eqs. (7) and (8):

$$\frac{\partial x_n}{\partial t} = f_+(w_n) + f_-(w_{n-1}) \; . \tag{11}$$

This relates the motion of step n to *velocity functions* $f_\pm$ of the widths of the terrace in front $[f_+(w_n)]$ and behind $[f_-(w_{n-1})]$ the moving step. A straightforward linear stability analysis of (11) around the uniform step train configuration with terrace width w shows[1] that if

$$f'_-(w) > f'_+(w), \tag{12}$$

the uniform step train is unstable towards step bunching. Here $f'_\pm$ are the derivatives of $f_\pm$.

4.2 Back terrace instability

While explicit expressions for the $f_\pm$ can be derived from the generalized BCF model, many essential features for the electromigration experiments seem to be captured by a simple *linear* model where

$$f^L_\pm(w) = k_\pm w \; . \tag{13}$$

This should be a reasonable approximation when the diffusion length is much larger than typical terrace widths and when the step motion is attachment/detachment limited, as is thought to be the case for Si[41]. This approximation also requires that steps are not so close together that direct entropic or elastic step-step interactions are important. When the asymmetry is such that the step velocity is more sensitive to processes associated with the terrace *in back of* the moving step, i.e., when $k_- > k_+$, Eq. (12) shows that the uniform step train is unstable towards step bunching. For concreteness, we refer to this as a *back-terrace asymmetry*. Note that a strong step edge barrier of the kind envisioned by Schwoebel[42] would yield such an asymmetry on any evaporating surface. However, we emphasize that the effective asymmetry in the velocity functions (13) can originate from a number of different microscopic processes. In particular, in the case of Si(111), the asymmetry is evidently a function of the electric field and the temperature.

4.3 Incorporating repulsive interactions

We assume that such an asymmetry is present in the electromigration experiments when the current is in the unstable direction. The resulting instability will cause some steps to come close to one another. When this happens, the repulsive interactions preventing step crossing must be taken into account and Eq. (13) is inadequate. An attempt to take account of the effects of step repulsions in the context of a generalized BCF model for general 2D step configurations leads to extremely complicated equations. To arrive at a simple 2D model capable of describing the appropriate physics both at large

[6] For a somewhat different approach that reaches the same conclusion, see Liu et al.[40]

and small step separations, we assume *weak coupling* between the different regimes and simply add the linear driving force terms $f_{\pm}^{L}(y)$ in Eq. (13) to the previously derived equations of motion (7) and (8) describing the effects of the repulsions. As with the treatment of repulsions, we evaluate the driving force terms in the 2D model using the same-y approximation.

Note that the $f_{\pm}$ incorporate both the general driving force leading to overall step motion as well as the source of the instability leading to step bunching. Of course in general one would expect that cross terms describing modifications of the repulsive interactions due to the driving force should arise. However, we believe the simple weak coupling approximation, which prevents step crossing at small separations and which incorporates the fundamental step bunching instability at large separations, will capture the essential physics on large length scales.

We have considered two limiting cases for the kinetics arising from the repulsive interactions in Eqs. (7) and (8). Hence in principle we will find two different model equations for the electromigration experiments when the driving force terms are added. However, as we will see, several basic features of the resulting models are independent of the kinetics when the system is driven far from equilibrium.

4.4 Case A

The simplest model equation capable of describing the electromigration experiments arises from Case A (non local mass flow) by adding the driving force term to Eq. (7). Thus we find our basic result:

$$\frac{\partial x_n(y)}{\partial t} = \frac{\Gamma_A}{\Omega k_B T}\mu_n(y) + k_+ w_n(y) + k_- w_{n-1}(y). \quad (14)$$

Using Eq. (6) this can be written in the 2D velocity function form originally suggested by KW[39]:

$$\frac{\partial x_n(y)}{\partial t} = \frac{\Gamma_A\ \tilde{\beta}}{k_B T}\frac{\partial^2 x_n(y)}{\partial y^2} + f_+^A(w_n(y)) + f_-^A(w_{n-1}(y)), \quad (15)$$

where

$$f_+^A(w) = -\frac{2\Gamma_A g}{k_B T}\left(\frac{1}{w^3}\right) + k_+ w,$$
$$f_-^A(w) = +\frac{2\Gamma_A g}{k_B T}\left(\frac{1}{w^3}\right) + k_- w. \quad (16)$$

Each $f_{\pm}^A(w)$ in Eq. (16) contains a short ranged direct interaction part preventing step crossing and a long ranged (linear) part describing the effects of diffusion and evaporation. More complicated expressions could be used for each part but we expect much the same qualitative features. For concreteness, we study here the case of evaporation so that the terrace ascends as the step index n increases. The following discussion can also be applied to the growth problem with some straightforward adjustments.

Note that the repulsive step interactions (which generate the short ranged terms proportional to g in $f_{\pm}^A$) do not change the *total* evaporation rate because on average they cancel each other when summed over all terraces. When the linear approximation is accurate for the $f_{\pm}$ at larger separations, an even stronger statement can be made. Using Eq. (15) and summing over all terraces, the average velocity of the steps is $(k_+ + k_-)w_a$ where w_a is the average terrace width. The total evaporation rate is then $(k_+ + k_-)$, which is a constant independent of both the average miscut angle and all surface configurations.

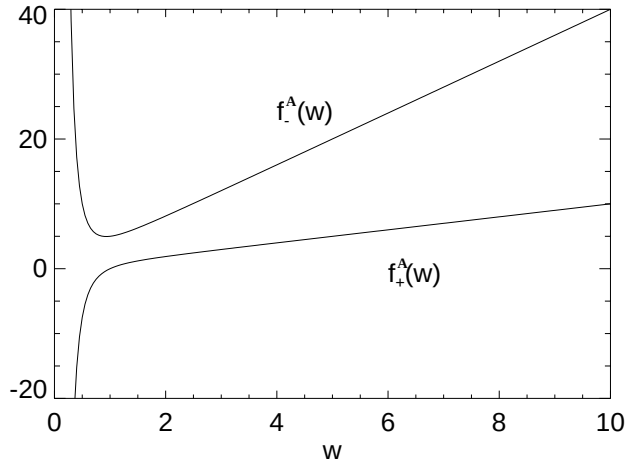

FIG. 4. Velocity functions in Case A given by Eq. (16). The parameters used are: $k_+ = 1$, $k_- = 4$, $G = 2\Gamma_a g/k_B T = 1$, $\gamma = 1$ and $w_a = 5$. Parameters are in arbitrary units.

With this simplification of the two dimensional step flow problem, we can study the long time behavior of the step train well beyond the initial onset of instability. We start with an array of 40 steps with small perturbations from an initial uniform configuration. We discretize the y coordinate so that each step has 2000 segments. Periodic boundary conditions are used in x and y direction. The time evolution problem of Eqs. (15) using (16) is converted into a set of difference equations. We control the time step so that during any time interval, each step moves only a small amount compared with its neighboring terrace widths. The segment size in the y direction is chosen small enough that the curvature is meaningful but is still large enough to include many features. As in KW[39], we are mainly interested in cases where k_+ and k_- are both positive. As an example we choose $k_+ = 1$,

$k_- = 4$, $G \equiv 2\Gamma_a g/k_B T = 1$, $\gamma \equiv \Gamma_A \tilde{\beta}/k_B T = 1$ and $w_a = 5$. The velocity functions $f_\pm$ given by Eq. (16) with these parameter values are shown in Fig. 4. These parameter values make the effect of direct repulsive interactions very small when steps are separated by the initial spacing w_a.

After the initial pairing instability, some of the steps come much closer to each other and the short ranged interaction terms become important. As the system continues to evolve, step bunches and single *crossing steps*, which leave one bunch and join another, begin to emerge. Thus there is also an instability toward *step debunching* in this model! The crossing steps move at a higher velocity than the step bunches. As successive crossing steps continually escape from the bunch behind and reattach to the bunch in front they usually form nearly equally spaced *crossing arrays* that connect two adjacent step bunches. Fig. 5 shows a snapshot of a system after about 140 monolayers are evaporated. The system continues to coarsen (the bunches gets bigger) until finite size effects become important. The coarsening can happen through the eating away of smaller bunches by debunching or through the merging of neighboring bunches. These patterns have a striking qualitative resemblance to the experimental results. Indeed, quantitative comparisons can be made[43], but this is outside the scope of the present work.

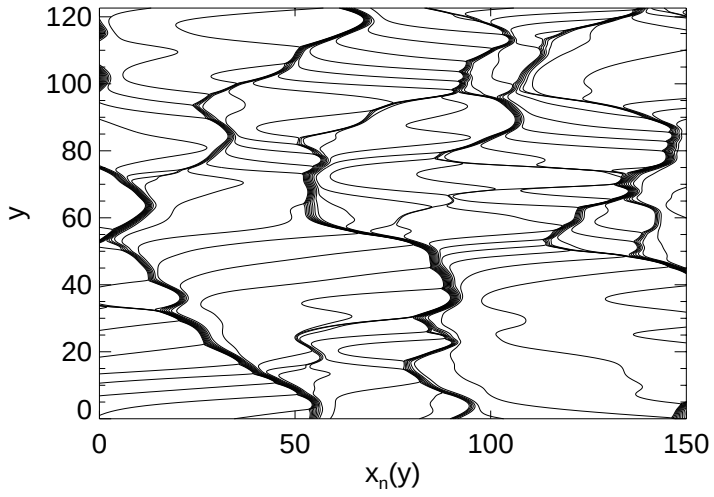

FIG. 5. A snapshot of a system of 40 steps after 140 monolayers are evaporated using Case A dynamics. The same parameters as in Fig. 5 are used. Steps flow from left to right. Only a portion of the system is shown.

4.5 Debunching instability

The origin of the debunching instability can be understood by considering a group of N_b straight step that are very close to each other and flanked by two very large terraces on each side with widths $w^{(b)}$ and $w^{(f)}$ respectively. The velocity of the step bunch is mainly determined by the width of the large terrace *behind* the step bunch. Defining the average position of the bunch as $X(y) = \sum_{n=1}^{N_b} x_n(y)/N_b$, then from Eqs. (15) and (16) we have

$$\partial X(y)/\partial t \approx \frac{1}{N_b}\left(f_-^L(w^{(b)}) + f_+^L(w^{(f)})\right), \qquad (17)$$

if we ignore the repulsion from other distant isolated steps and if the width of the step bunch itself is much smaller than the widths of the flanking terraces. The velocity of the first step in the bunch is always larger than $f_+^L(w^{(f)})$ (the other term $f_-^L(w^{(b)})$ is always positive), and hence when $w^{(f)}$ is large enough, the first step's velocity can be *larger* than the average velocity of the bunch, which from Eq. (17) *decreases* as the bunch size increases. Thus the first step can eventually *escape* from the bunch. This leads to the debunching, and the subsequent formation of crossing arrays.

These same features have been observed in the Monte Carlo simulations of the model of KW[39], in which the direct step interactions are treated through the imposition of a minimum distance constraint and allowing multistep jumps. The same long-ranged (linear) velocity functions were used in that model. Both the dynamical behavior and the patterns formed are very similar in the two models. We conclude that the details of the short ranged interactions are not important for the creation of step bunches and crossing arrays in this kind of a model. Indeed, we have verified that modifying the form of the repulsive interaction in Eq. (16) does not change the basic features as long as the interaction is a short ranged repulsion that prevents step overhangs. As would be expected, the main differences are in the details of the step profile in the step bunch. See Lui *et al.*[40,49] for further discussion.

4.6 Case B

The persistence of these basic features is perhaps most dramatically illustrated by considering the more complicated case that arises when the effects of the repulsions are treated with locally conserved dynamics (Case B). Adding the driving force term Eq. (13) to Eq. (8) yields the new electromigration model

$$\frac{\partial x_n(y)}{\partial t} = \frac{\Gamma_B}{\Omega k_B T}[\{\mu_n(y) - \mu_{n+1}(y)\} + \{\mu_n(y) - \mu_{n-1}(y)\}] + k_+ w_n(y) + k_- w_{n-1}(y). \qquad (18)$$

We can write this in a general velocity function form

$$\frac{\partial x_n}{\partial t} = f_+(\mu_n, \mu_{n+1}, w_n) + f_-(\mu_{n-1}, \mu_n, w_{n-1}), \quad (19)$$

but we see that in this case each $f_\pm$ directly couples *four* steps together, rather than two as in the nonconserved case.

Equations similar to (18) could arise from generalizations to 2D of models considered by Uwaha *et al.*[44,45] and Natori[46]. These authors modified the one dimensional BCF model to include direct step interactions, which can affect the adatom chemical potential at the step edges[2,3] (or the equilibrium adatom concentration near the steps). All step motion was still assumed to arise from the modified diffusion fields, so local mass conservation is satisfied. The diffusion fields were determined using the quasistatic approximation. Note that this approximation is less justified when steps are interacting strongly since their velocity may not be very slow compared with the diffusion field[47,48]. They found interesting dynamical behavior in a number of different cases, including some effects of step debunching.

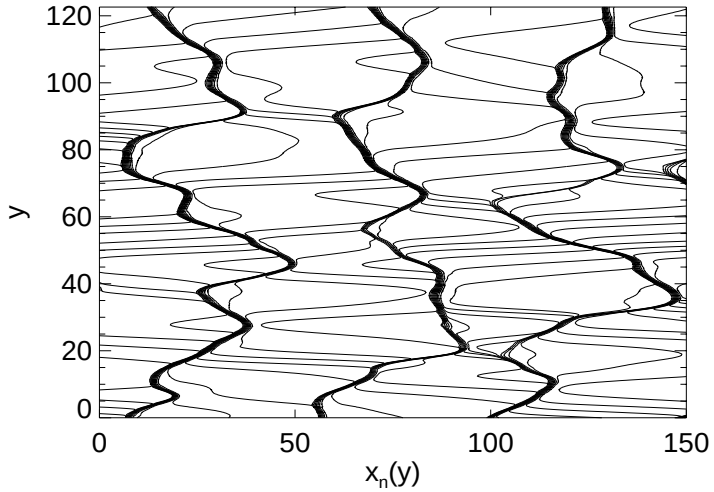

FIG. 6. A snapshot of a system of the same size as in Fig. 6 but using Case B dynamics. Parameters used here: $k_+ = 1$, $k_- = 4$, $G = 2\Gamma_b g/k_B T = 1$, $\gamma = \Gamma_b \tilde{\beta}/k_B T = 1$ and $w_a = 5$.

The time evolution of a 2D step array given by Eq. (19) can be again solved for numerically. We find that the basic features are the same as in the nonconserved case. Fig. 6 shows a snap shot of the system using the same anisotropy ratio $k_+/k_- = 4$ as in Fig. 5. We observe again that when there is enough driving force to move the system far away from equilibrium, the details of how we treat the step interactions are not very important for the formation of the basic crossing array patterns. Quantitative comparison of the two models with each other and with experiment will be given elsewhere[40,49].

In conclusion, the patterns generated by KW[39] seem to arise naturally in 2D systems with unstable step flow resulting from a back-terrace instability. We are able to reproduce most of KW's results by simply modifying the velocity functions at short distances to incorporate the effects of step repulsions, as suggested by the weak coupling picture. These compare favorably with experiments on current induced step bunching in Si(111)[8–10,43]. Other physical limits, e.g., local mass conservation, can be incorporated with some generalization of the forms of the velocity functions.

Acknowledgements: Part of this work was done in collaboration with Daniel Kandel and Ellen Williams, who we also thank for many helpful discussions. We also thank Ted Einstein and Norm Bartelt for useful remarks. This work was supported by the NSF-MRG with continuing support from the NSF-MRSEC under contract DMR-96-32521.

REFERENCES

1. P. Bennema and G. H. Gilmer, in *Crystal Growth: An Introduction*, p. 263, P. Hartman, ed., North Holland, Amsterdam, (1973).
2. P. Nozières, *J. Phys. France* 48:1605 (1987).
3. A. Rettori and J. Villain, *J. Phys. France* 49:257 (1988).
4. M. Ozdemir and A. Zangwill, *Phys. Rev. B* 42:5013 (1990).
5. N. Bartelt, T. Einstein, and E. Williams, *Surf. Sci.* 240:L591 (1990).
6. E. D. Williams, *Surf. Sci.* 299/300:502 (1994).
7. E. D. Williams and N. C. Bartelt, in *Handbook of Surface Science*, W. N. Unertl, ed., North-Holland, Amsterdam, (1996).
8. A. Latyshev, A. Aseev, A. Krasilnikov, and S. Stenin, *Surf. Sci.* 227:24 (1990).
9. A. Latyshev, A. Aseev, A. Krasilnikov, and S. Stenin, *Surf. Sci.* 213:157 (1989).
10. See, for example, Y. Homma, R. J. McClelland, and H. Hibino, *Jpn. J. Appl. Phys.* 29:L2254 (1990); H. Yasunaga, and A. Natori, *Surf. Sci. Rep.* 15:205 (1992) and references therein; M. J. Ramstad, R. J. Birgeneau, K. I. Blum, D. Y. Noh, B. O. Wells, and M. J. Young, *Europhys. Lett.* 24:653 (1993); A. V. Latyshev, A. B. Krasilnikov, and A. L. Aseev, *Surf. Sci.* 311:395 (1994).
11. R. J. Phaneuf, N. C. Bartelt, E. D. Williams, W. Święch, and E. Bauer, *Phys. Rev. Lett.* 67:2986 (1991).
12. J. S. Ozcomert, W. W. Pai, N. C. Bartelt, and J. E. Reutt-Robey, *Phys. Rev. Lett.* 72:258 (1994).
13. E. S. Fu, M. D. Johnson, D.-J. Liu, J. D. Weeks, and E. D. Williams, *Phys. Rev. Lett.* 77:1091 (1996).
14. D.-J. Liu, E. S. Fu, M. D. Johnson, J. D. Weeks, and E. Williams, *J. Vac. Sci. Technol. B* 14:2799 (1996).
15. B. Joós, T. L. Einstein, and N. C. Bartelt, *Phys. Rev. B* 43:8153 (1991).
16. E. E. Gruber and W. W. Mullins, *J. Phys. Chem. Solids* 28:875 (1967).
17. For a general review, see R. Evans, in *Fundamentals of Inhomogeneous Fluids*, D. Henderson ed., Dekker, New York, (1992).
18. D.-J. Liu and J. D. Weeks (unpublished).

19. W. K. Burton, N. Cabrera, and F. C. Frank, *Proc. R. Soc. London, Ser. A* 243:299 (1951).
20. N. C. Bartelt, J. L. Goldberg, T. L. Einstein, and E. D. Williams, *Surf. Sci.* 273:252 (1992).
21. N. C. Bartelt, T. L. Einstein, and E. D. Williams, *Surf. Sci.* 276:308 (1992).
22. M. Yoon, S. G. J. Mochrie, D. M. Zehner, G. M. Watson, and D. Gibbs, *Surf. Sci.* 338:225 (1995).
23. F. Pourmir, S. Rousset, S. Gauthier, M. Sotto, J. Klein, and J. Lecoeur, *Surf. Sci.* 324:L337 (1995).
24. F. Katsuki and K. Kamei, *Applied Surface Science* 94/95:485 (1996).
25. H.-C. Jeong and J. D. Weeks, *Phys. Rev. Lett.* 75:4456 (1995).
26. D.-J. Liu, J. D. Weeks, M. D. Johnson, and E. D. Williams, *Phys. Rev. B* (in press).
27. R. J. Phaneuf, N. C. Bartelt, E. D. Williams, W. Święch, and E. Bauer, *Phys. Rev. Lett.* 71:2284 (1993).
28. H.-C. Jeong and J. D. Weeks (unpublished).
29. H. Hibino, Y. Homma, and T. Ogino, *Phys. Rev. B* 51:7753 (1995).
30. J. R. Heffelfinger, M. W. Bench, and C. B. Carter, *Surf. Sci.* 343:L1161 (1995).
31. W. W. Mullins, *J. Appl. Phys.* 28:333 (1957).
32. K. Hata *et al.*, *Appl. Phys. Lett.* 76:5601 (1994).
33. M. Suzuki, Y. Homma, Y. Kudoh, and R. Kaneko, *Ultramicroscopy* 42-44:940 (1992).
34. C. Misbah, O. Piere-Louis, and A. Pimpinelli, *Phys. Rev. B* 51:17283 (1995).
35. S. Stoyanov, *Jpn. J. Appl. Phys.* 30:1 (1991).
36. S. Stoyanov, *Applied Surface Science* 60/61:55 (1992).
37. S. S. Stoyanov, H. Nakahara, and M. Ichikawa, *Jpn. J. Appl. Phys.* 33:254 (1994).
38. D. Kandel and E. Kaxiras, *Phys. Rev. Lett.* 76:1114 (1996).
39. D. Kandel and J. D. Weeks, *Phys. Rev. Lett.* 74:3632 (1995).
40. D.-J. Liu, J. D. Weeks, and D. Kandel, *Surf. Rev. and Lett.* (in press).
41. Y.-N. Yang and E. Williams, *Phys. Rev. Lett.* 72:1862 (1994).
42. R. L. Schwoebel and E. J. Shipsey, *J. Appl. Phys.* 37:3682 (1966).
43. E. D. Williams, E. Fu, Y.-N. Yang, D. Kandel, and J. D. Weeks, *Surf. Sci.* 336:L746 (1995).
44. M. Uwaha, *J. Crystal Growth* 128:92 (1993).
45. M. Uwaha, Y. Saito, and M. Sato, *J. of Crys. Growth* 146:164 (1995).
46. A. Natori, *Jpn. J. Appl. Phys.* 33:3538 (1994).
47. R. Ghez and S. S. Iyer, *IBM J. Res. Dev.* 32:804 (1988).
48. F. Liu and H. Metiu, *Phys. Rev. E* 49:2601 (1994).
49. D.-J. Liu, J. D. Weeks, and D. Kandel (unpublished).